^{18}F-fluorodeoxyglucose positron emission tomography for the detection of inflammatory lesions of the arterial vessel walls in Wistar rats

SHIWEI SHEN[1*], HONGWEI LI[2*], SONG GE[3*], HONGBO HUANG[4], HUI ZHANG[5], FENG LI[6], YINBO FENG[7], LING WANG[6], XIAOFENG WENG[8], YUN LU[6] and ZHENHAI SHEN[6]

[1]Department of Endocrinology, Wuxi No. 2 People's Hospital Affiliated to Nanjing Medical University, Wuxi, Jiangsu 214002; [2]Department of Rehabilitation, Jiangsu Provincial Research Center for Health Assessment and Intervention, Jiangsu Provincial Taihu Sanatorium, Wuxi, Jiangsu 214086; [3]Department of Neurology, The First Affiliated Hospital of Nanjing Medical University, Nanjing, Jiangsu 210029; [4]Micro PET Center, Jiangsu Institution of Nuclear Medicine, Wuxi, Jiangsu 214063; [5]Cardiovascular Surgery, The First Affiliated Hospital of Nanjing Medical University, Nanjing, Jiangsu 210029; [6]Internal Medicine, [7]Department of Radiology and [8]Clinical Laboratory, Jiangsu Provincial Research Center for Health Assessment and Intervention, Jiangsu Provincial Taihu Sanatorium, Wuxi, Jiangsu 214086, P.R. China

Abstract. The present study aimed to evaluate the use of ^{18}F-fluorodeoxyglucose (^{18}F-FDG) positron emission tomography (PET) for detection of high-fat and high-salt diet-induced inflammatory lesions of the arterial vessel walls in Wistar rats. A total of 20 healthy, 8-week-old, male Wistar rats were randomly assigned to the high-fat diet group and the normal diet group. After 16 and 24 weeks of feeding, Wistar rats in the normal diet group and the high-fat diet group (five rats in each group) were injected with ^{18}F-FDG through the tail vein at a dose of 1 mCi/kg after fasting for 12 h. After 1 h, the rats were anesthetized with 2% isoflurane, followed by micro-PET imaging with a 10-min image capture duration and immunohistochemical staining. The standardized uptake values (SUVs) of ^{18}F-FDG were significantly higher in the iliac artery in the high-fat diet group compared with those in the normal diet group at 16 weeks (1.53±0.08 vs. 1.04±0.03; P<0.05) and at 24 weeks (1.96±0.17 vs. 1.12±0.07; P<0.05). The SUVs of ^{18}F-FDG were also significantly greater in the abdominal aorta in the high-fat diet group compared with those in the normal diet group at 16 weeks (1.35±0.08 vs. 1.02±0.02; P<0.05) and at 24 weeks (1.54±0.09 vs. 1.04±0.02; P<0.05). In addition, the SUVs of ^{18}F-FDG in the iliac artery and abdominal aorta were significantly higher at 24 weeks compared with those at 16 weeks in the high-fat diet group (P<0.05). As determined by immunohistochemistry, the percentage of CD68-positive cells in the total number of cells per unit area in each group was 3.20±1.80% in the 24-week normal diet group, 4.70±2.02% in the 16-week high-fat diet group and 6.94±2.02% in the 24-week high-fat diet group; the percentage of CD68-positive cells in the high-fat diet group at 24 weeks was significantly higher than that in the high-fat diet group at 16 weeks and in the normal diet group at 24 weeks (P<0.05). In conclusion, ^{18}F-FDG PET is a noninvasive imaging tool that can continuously monitor inflammatory lesions of the arterial vessel walls in Wistar rats. Further improvement of the Wistar rat atherosclerosis model may provide data to support the early assessment of and intervention in atherosclerosis.

Correspondence to: Dr Yun Lu or Dr Zhenhai Shen, Internal Medicine, Jiangsu Provincial Research Center for Health Assessment and Intervention, Jiangsu Provincial Taihu Sanatorium, 1 Shenggan Road, Yuantouzhu Park, Wuxi, Jiangsu 214086, P.R. China
E-mail: shentaihu2017@126.com
E-mail: shentaihu2030@126.com

*Contributed equally

Introduction

With population aging and lifestyle changes, the incidence of atherosclerotic cardiovascular disease continues to rise (1). It was estimated that the number of patients with cardiovascular diseases was 422.7 million globally in 2015 (2). In China, the number of patients with cardiovascular diseases was >290 million in 2015, and such diseases have become a major cause of death in Chinese populations (1).

The current available approaches, such as angiography and intravascular ultrasound, have shown diagnostic value for atherosclerosis; however, these tools are all invasive, and are not of diagnostic significance until the atherosclerotic plaques are large enough or the vascular stenosis is severe (3). A

search for novel, noninvasive approaches for diagnosis of early atherosclerosis is therefore of great importance for the assessment and management of atherosclerosis. Atherosclerosis is accepted as a chronic inflammatory disorder (4), and the monocyte-macrophage system has been shown to have a critical role in its development and progression (5,6). Uptake of ^{18}F-fluorodeoxyglucose (^{18}F-FDG) has been reported to be strongly associated with macrophage density. Chen *et al* (7) suggested that the standardized uptake values (SUVs) of ^{18}F-FDG may be closely associated with the number of macrophages, and indicated that ^{18}F-FDG positron emission tomography (^{18}F-FDG PET) imaging may be able to quantify the metabolic activity of macrophages in the rat arterial vessel walls under various physiological or pathological conditions. In addition, ^{18}F-FDG PET imaging may directly display local inflammation and the metabolic activity of macrophage accumulation in atherosclerosis, which may be used to assess early inflammation in atherosclerosis (8-10). The utility of ^{18}F-FDG PET as a marker of inflammation has been extensively studied in mouse and rabbit models of atherosclerosis, as well as in humans (11). The purpose of the present study was to design a Wistar rat model of high-fat and high-salt diet-induced inflammatory lesions of the arterial vessel walls, in order to evaluate the value of ^{18}F-FDG PET, as a noninvasive tool, in the assessment and management of early inflammation in atherosclerosis. These findings could be of great clinical significance for early diagnosis, assessment and treatment of early atherosclerotic diseases.

Materials and methods

Modeling inflammatory lesions of the arterial vessel walls in rats. A total of 20 healthy 8-week-old male rats (230-250 g) of the Wistar strain were purchased from the Comparative Medicine Center of Yangzhou University (Yangzhou, China). After adaptive feeding for a week in the laboratory, rats were randomly grouped, with 10 animals in each group. Rats in the normal diet group (n=10) were given conventional rodent feed (10% fat, 22% protein, 68% carbohydrate and 0.5% salt; Shanghai SLAC Laboratory Animal Co., Ltd.), whereas rats in the high-fat diet group (n=10) consumed high-fat and high-salt feed (49% fat, 21% protein, 30% carbohydrate and 2% salt; Shanghai SLAC Laboratory Animal Co., Ltd.) for 16-24 weeks. All rats were caged and given free access to food and water. All animals were housed in a facility at room temperature (18-26˚C) and ~50% humidity under a 12/12-h light/dark cycle. Rats were fed in the morning and evening each day, and the water was changed every other day. Body weight, body length and abdominal circumference were measured once every 4 weeks, and blood pressure, heart rate, blood lipid, blood glucose and insulin (INS) levels were measured once every 8 weeks.

Measurement of blood pressure. Rat blood pressure was measured using a rat-tail artery blood pressure test system (BP-98A meter; Softron Beijing Biotechnology Co., Ltd; http://www.softron.cn/). All rats were kept in an incubator at 37˚C for 5 min before the measurement. During the measurement, all animals were kept awake, with limited activity. Each rat was measured twice, and the mean blood pressure was calculated. Meanwhile, the rat heart rates were monitored during the blood pressure measurement.

Measurement of body weight, body length and abdominal circumference. The rat body weight was measured via the conventional method, using an electronic balance with an accuracy of 0.1 g to measure the weight of each rat. When the data became stable, the readout was recorded. Abdominal circumference (cm) was assessed on the largest zone of the rat abdomen using a plastic non-extensible measuring tape, and body length was defined as the length between the nose and anus. Lee's index was calculated as follows: Lee's index = [body weight (g)]x1/3x[103/body length (cm)].

Measurement of blood lipids, blood glucose and INS levels. After fasting for 12 h, blood samples (0.5-1.0 ml) were collected by cutting the rat tail. The blood glucose level was measured using a ONETOUCH® UltraVue™ glucose meter (LifeScan, LLP), and the triglyceride (TG), total cholesterol (TC), high-density lipoprotein cholesterol (HDL-C) and low-density lipoprotein cholesterol (LDL-C) levels were tested with commercial reagents (Wako Pure Chemical Industries, Ltd.) on a Hitachi 7600 fully automatic biochemical analyzer (Hitachi, Ltd.). Blood INS concentration was measured with commercial reagents (Beckman Coulter, Inc.) on a DxI 800 Access Immunoassay system (Beckman Coulter, Inc.). All measurements were performed according to the manufacturers' instructions. Rats were anesthetized with 400 mg/kg chloral hydrate (Sinopac Chemical Reagent Co., Ltd.). Before use, a 4% chloral hydrate solution was prepared using 0.9% sodium chloride and subsequently it was intraperitoneally injected to the rats. If rats lost >15% of their body weight or could not eat for >3 days, rats were euthanized by cervical dislocation. However, none of the rats reached the humane endpoints early in the study.

^{18}F-FDG micro-PET imaging. A total of 16 and 24 weeks after feeding, Wistar rats in the normal diet group and the high-fat diet group (n=5 rats/group) were injected with ^{18}F-FDG (supplied by the Department of Nuclear medicine, Affiliated Hospital of Jiangnan University, Wuxi, China; http://www.wuxihospital.com/petct/index.html) through the tail vein at a dose of 1 mCi/kg after fasting for 12 h. After 1 h, 2% isoflurane (Minrad International, Inc.) was used to induce anesthesia in rats and anesthesia was maintained with 1.5% isoflurane (12,13) using a Midmark Matrx anesthesia machine (Midmark Corporation). Subsequently, micro-PET imaging was performed using a Siemens Inveon micro-PET scanner (Siemens Healthineers) with an LSO crystal; the conditions were as follows: Death time of 40 nsec, a 20x20 matrix, a 1.4-mm maximum resolution of the imaging field of view, a detection range of 10x10x12.7 cm, a slice thickness of 0.8 mm, and a 10-min image capture duration. To ensure consistency between the micro-PET scanning slices and the pathological sections, the blood vessels in the inferior segment of the abdominal aorta that were proximal to the bilateral iliac artery bifurcation were sampled for micro-PET scanning.

Pathological examinations. After micro-PET imaging, rats were intraperitoneally injected with chloral hydrate

(400 mg/kg) for anesthesia (14,15), and euthanized by cardiac perfusion with normal saline and 4% paraformaldehyde. Death was confirmed by cardiac and respiratory arrest. The abdominal aorta and the bilateral iliac artery were then dissected, and the blood vessels in the inferior segment of the abdominal aorta that were proximal to the bilateral iliac artery bifurcation were collected. Blood vessels were fixed in 4% paraformaldehyde (4˚C; 12 h), dehydrated in a gradient ethanol series and embedded in paraffin wax at 25˚C overnight. The duration of the experiment lasted for ~1 h. Subsequently, the vascular cross sections were sectioned into 4-μm thick slices. For immunohistochemistry, vascular sections were incubated with a primary antibody against CD68 (1:1,000; cat. no. ab125212; Abcam) at 4˚C overnight, followed by incubation with an HRP-conjugated secondary antibody (1:2,000; cat. no. 8114; Cell Signaling Technology, Inc.) for 1 h at room temperature, detected with 3,3'-diaminobenzidine at 25˚C for 20 min, and counterstained with hematoxylin. The slides were examined using Olympus microscope (BX41) and Olympus DP70 Digital Camera System at x200 magnification (Olympus Corporation). The brown-stained area (CD68+ cells) was separately quantified using ImageJ version 1.52a (National Institutes of Health).

Ethical considerations. All animal studies were conducted in accordance with the recommendations in the Guidelines for the management and use of laboratory animals (16) The present study was approved by the Ethics Review Committee of Jiangsu Lake Taihu Sanatorium (permission no. SGLERC-2011008; Wuxi, China) and Jiangsu Provincial People's Hospital Group (permission no. SRY20100820).

Data analyses. The region of interest (ROI) of high ^{18}F-FDG uptake in the blood vessels was marked using the ASI Pro VM™ MicroPET Analysis software version 6.8.6.9 (Concorde Microsystems, Inc.) and the ^{18}F-FDG SUVs were calculated using the following formula: SUV mean (the average of uptake within the ROI) = (radioactivity concentration in ROI x rat body weight)/total administered dose of ^{18}F-FDG (decay corrected).

Independent samples t-test was used to assess the differences in physiological indexes and metabolic parameters between the groups. In addition, comparison of SUV values between the different groups over the same period was made using the independent samples t-test. Considering the influence of time and sample size, the Mann-Whitney U test was used to compare SUV values at weeks 16 and 24 in the high-fat group. The differences in CD68 staining intensity among groups were analyzed by one-way ANOVA followed by Tukey's post hoc test. The data are presented as the mean ± SEM and box-and-whisker diagrams in Figs. 1-3. All statistical analyses were conducted using SPSS statistical software, version 15.0 (SPSS, Inc.). P<0.05 was considered to indicate a statistically significant difference.

Results

Changes in physical and metabolic parameters. As shown in Table I, there were no significant differences between the normal diet group and the high-fat diet group in terms of body weight, abdominal circumference, body length, Lee's index
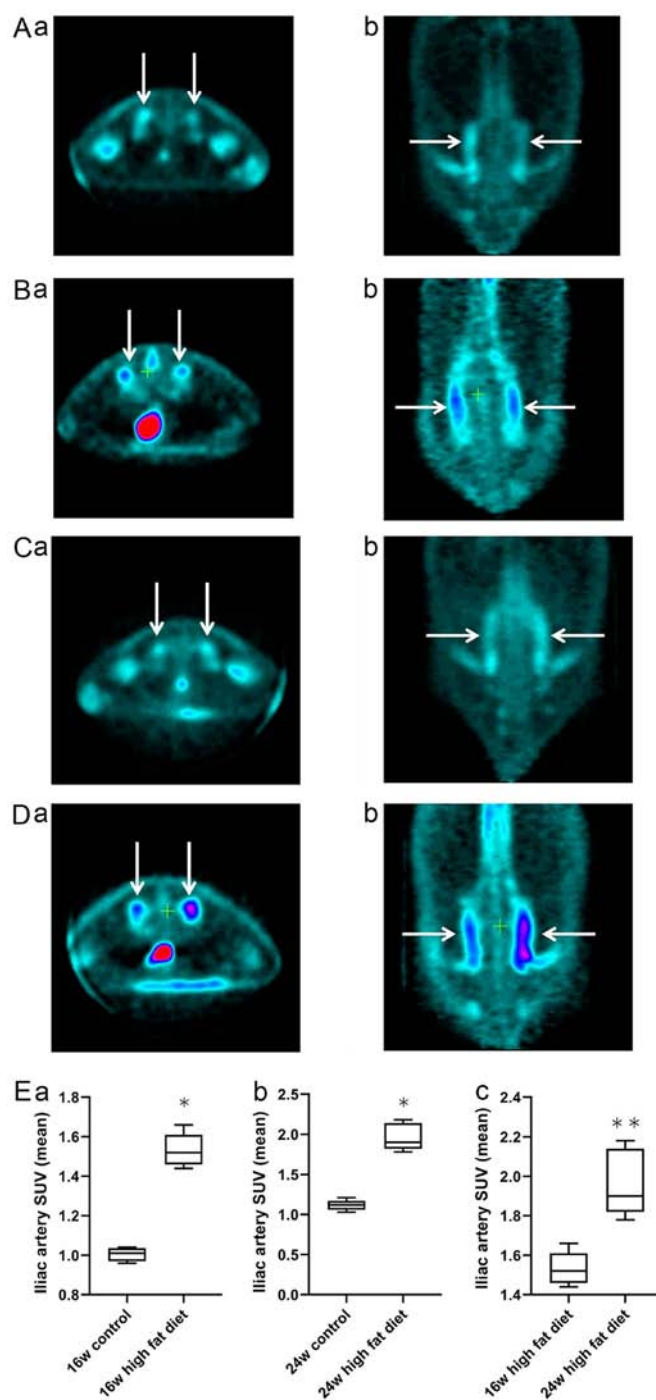

Figure 1. Uptake of ^{18}F-FDG into the bilateral iliac arteries of rats on a normal diet and a high-fat diet at 16 and 24 weeks. (Aa and Ab) Normal diet group at 16 weeks, (Ba and Bb) high-fat diet group at 16 weeks. (Ca and Cb) Normal diet group at 24 weeks, (Da and Db) high-fat diet group at 24 weeks. Arrows indicate the cross section (Aa, Ba, Ca and Da) and coronal plane (Ab, Bb, Cb and Db) of the vessels of the bilateral iliac artery. The magnification is 2. Comparison of the mean SUVs of bilateral iliac vascular uptake of ^{18}F-FDG at (Ea) 16 and (Eb) 24 weeks in the normal diet group and the high-fat diet group. *P<0.05 vs. the control group. (Ec) Comparison of the mean SUVs of bilateral iliac vascular uptake of ^{18}F-FDG at 16 and 24 weeks in the high-fat diet group.**P<0.01 vs. the 16-week high-fat diet group. ^{18}F-FDG, ^{18}F-fluorodeoxyglucose; SUV, standardized uptake value.

or blood pressure at baseline and after 8 weeks of feeding (P>0.05). Differences between groups were analyzed by independent samples t-test. The body weight and abdominal circumference were higher in the high-fat diet group compared

Table I. Changes in physical and metabolic parameters in rats.

Characteristic	Baseline Normal diet	Baseline High-fat diet	4 weeks Normal diet	4 weeks High-fat diet	8 weeks Normal diet	8 weeks High-fat diet	12 weeks Normal diet	12 weeks High-fat diet	16 weeks Normal diet	16 weeks High-fat diet	20 weeks Normal diet	20 weeks High-fat diet	24 weeks Normal diet	24 weeks High-fat diet
Weight (g)	241.20±17.04	238.71±18.53	318.52±34.51	315.47±43.48	363.08±42.20	418.18±63.49[a]	377.05±62.27	463.75±68.38[b]	410.09±59.33	528.59±92.26[b]	429.76±64.29	585.69±83.05[b]	453.86±57.22	614.00±121.83[b]
Body length (cm)	20.97±1.34	20.73±0.96	22.4±1.24	22.18±1.73	23.39±1.05	23.89±1.41	24.70±1.09	24.04±1.68	24.35±1.27	24.95±1.25	24.57±1.40	25.88±1.30	25.76±0.89	25.43±2.30
Abdominal circumference (cm)	16.20±0.63	16.36±0.85	17.85±1.23	18.18±0.97	18.35±0.75	19.24±0.71[b]	18.05±1.14	19.82±1.01[b]	19.00±2.21	20.92±1.88[a]	20.07±1.17	21.75±1.60[a]	21.21±0.91	23.14±1.07[b]
Lee's index	297.59±17.00	299.54±12.41	304.91±10.61	307.18±13.83	304.65±4.25	312.41±6.15[b]	306.80±39.29	321.80±10.62	304.79±16.39	322.98±13.93[a]	306.68±12.08	322.89±11.23[a]	303.89±11.62	333.90±17.32[b]
HR (bpm)	377.9±24.55	362.43±13.52	~	~	371.80±42.37	406.29±45.82	372.60±29.95	375.21±46.00	365.80±66.99	399.25±30.38	386.71±37.66	397.50±43.82	401.5±42.95	413.71±26.65
SBP (mmHg)	116.40±9.79	113.14±7.12	~	~	117.90±13.54	126.00±16.30	120.80±6.88	138.21±14.43[b]	106.00±15.98	141.17±21.61[b]	112.57±13.11	142.33±26.29[a]	102.33±24.65	145.00±17.17[b]
DBP (mmHg)	76.60±5.35	69.57±7.56[a]	~	~	86.50±11.92	89.64±17.93	77.70±11.00	104.36±15.44[b]	75.10±16.48	106.50±22.37[b]	74.29±10.77	98.33±11.71[b]	74.83±11.97	92.43±20.25[a]
TG (mmol/l)	0.38±0.16	0.39±0.09	~	~	1.43±0.59	1.04±0.87	~	~	1.46±0.32	2.02±0.51	~	~	1.53±0.39	1.44±0.63
TC (mmol/l)	1.79±0.31	1.71±0.44	~	~	1.69±0.14	2.21±0.33[b]	~	~	1.51±0.36	2.02±0.47	~	~	1.57±0.44	2.31±0.45[a]
HDL-C (mmol/l)	0.94±0.13	0.96±0.31	~	~	0.86±0.09	0.85±0.23	~	~	0.99±0.18	0.97±0.22	~	~	0.96±0.24	1.05±0.33
LDL-C (mmol/l)	0.68±0.09	0.67±0.20	~	~	0.69±0.21	0.72±0.30	~	~	0.67±0.09	0.89±0.09[a]	~	~	0.81±0.23	0.61±0.46
FBG (mmol/l)	4.98±0.44	4.66±0.63	~	~	4.83±0.44	5.13±0.39	~	~	5.32±0.56	4.84±0.20	~	~	4.97±0.36	5.55±0.58
INS (μU/ml)	0.11±0.06	0.13±0.17	~	~	0.19±0.13	0.17±0.14	~	~	0.14±0.05	0.12±0.04	~	~	0.08±0.03	0.19±0.09[a]

[a]$P<0.05$, [b]$P<0.01$ vs. normal diet group. HR, heart rate; SBP, systolic blood pressure; DBP, diastolic blood pressure; TG, triglyceride; TC, total cholesterol; LDL-C, low density lipoprotein cholesterol; HDL-C, high density lipoprotein cholesterol; FBG, fasting blood glucose; INS, insulin; bpm, beats per minute.

with those in the normal diet group at 8 weeks (P<0.05), and the systolic blood pressure (SBP) and diastolic blood pressure (DBP) were higher in the high-fat diet group compared with those in the normal diet group at 12 weeks (P<0.05). There was no significant difference in heart rate between the two groups (P>0.05) (Table I).

There were no significant differences in the INS levels between the two groups at baseline, and at 8 and 16 weeks (P>0.05). However, higher INS levels were detected in the high-fat diet group compared with those in the normal diet group at 24 weeks (P<0.05). Higher TC concentrations were detected in the high-fat diet group compared with those in the normal diet group at 8 and 24 weeks (P<0.05), and a higher LDL-C concentration was revealed in the high-fat diet group compared with that in the normal diet group at 16 weeks (P<0.05). No significant differences were observed between the two groups in terms of fasting glucose concentration, TG or HDL-C levels (P>0.05) (Table I).

^{18}F-FDG micro-PET imaging of rats. The cross-sectional and coronal profiles of ^{18}F-FDG uptake by bilateral iliac arteries at weeks 16 and 24 in rats in the normal diet group (Fig. 1Aa, b, Ca and b) and high-fat diet group (Fig. 1Ba, b, Da and b) are shown. Independent samples t-test was used for analysis of the normal diet and high-fat diet groups. At week 16, the mean SUV of ^{18}F-FDG in the iliac artery vessels in the high-fat diet group was significantly higher than that in the normal diet group (1.53±0.08 vs. 1.04±0.03; P<0.05; Fig. 1Ea). At week 24, the mean SUV of ^{18}F-FDG in the iliac artery vessels in the high-fat diet group was significantly higher than that in the normal diet group (1.96±0.17 vs. 1.11±0.07; P<0.05; Fig. 1Eb). For analysis of rats in the high-fat diet group at weeks 16 and 24, a Mann-Whitney U test was used. The average SUV intake of ^{18}F-FDG in the iliac artery at week 24 was significantly higher than that at week 16 in the high-fat diet group (1.96±0.17 vs. 1.53±0.08; P<0.01; Fig. 1Ec). These results indicated that the uptake of ^{18}F-FDG into the iliac artery wall was significantly increased in rats on a high-fat diet with increased feeding time.

The sagittal plane of ^{18}F-FDG uptake by the abdominal aorta at weeks 16 and 24 in rats in the normal diet group (Fig. 2Aa and b) and high-fat diet group (Fig. 2Ba and b) are shown. Independent samples t-test was used for analysis of the normal diet and high-fat diet groups. At weeks 16 (1.35±0.08 vs. 1.02±0.02) and 24 (1.54±0.09 vs. 1.04±0.02), the mean SUV of ^{18}F-FDG in the abdominal aorta in the high-fat diet group was significantly higher than that in the normal diet group (all P<0.05; Fig. 2Ca and b). For analysis of rats in the high-fat diet group at weeks 16 and 24, a Mann-Whitney U test was used. The uptake of ^{18}F-FDG in the abdominal aorta in the high-fat diet group at week 24 was significantly higher than that at week 16 (1.54±0.09 vs. 1.35±0.08; P<0.05; Fig. 2Cc). These findings indicated that, with the increase in feeding time, the uptake of ^{18}F-FDG into the abdominal aortic wall of the rats on a high-fat diet was significantly increased.

CD68-positive cells. The expression of CD68-positive macrophages was detected in the abdominal aortic wall of rats (Fig. 3). Immunohistochemical staining of CD68 in the abdominal aortic vascular wall was conducted on rats in the
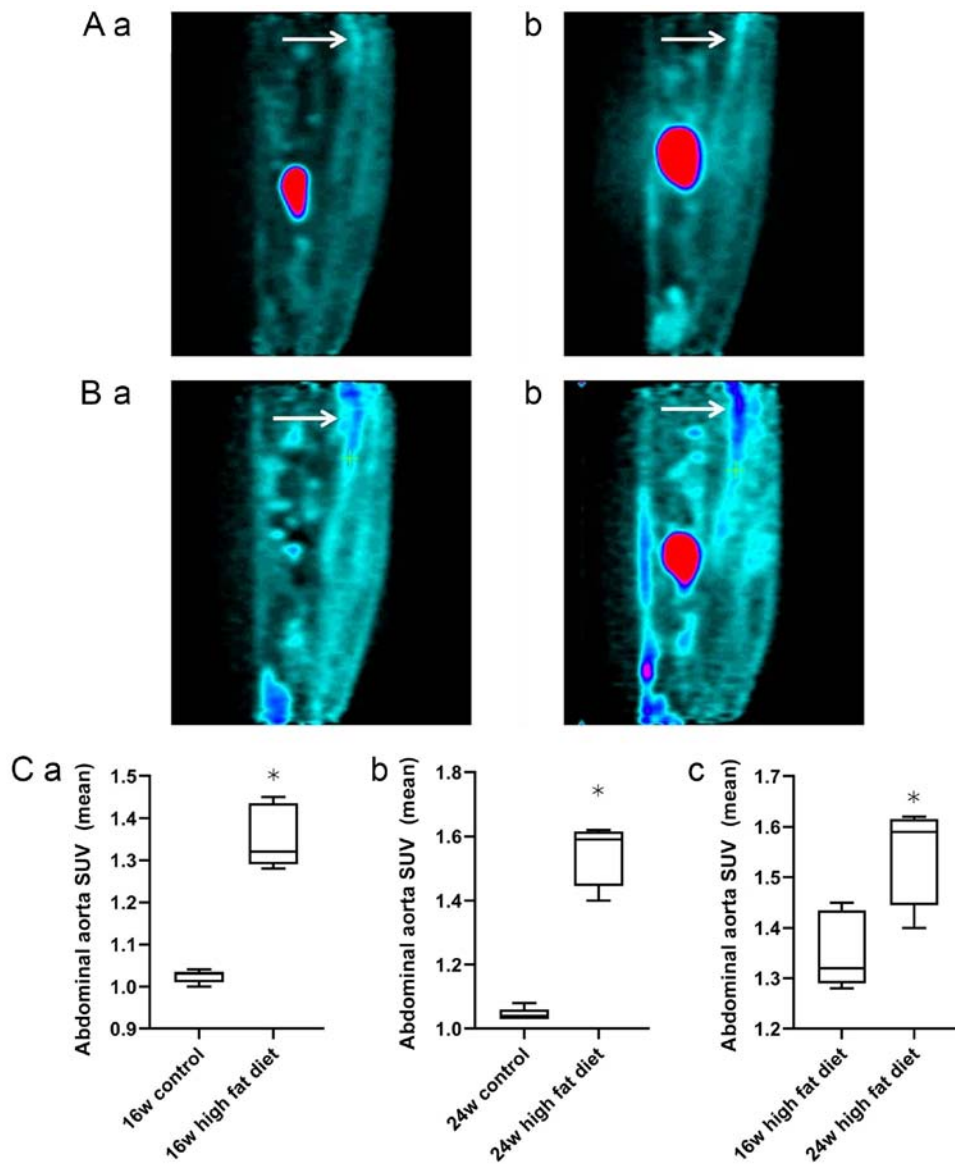
Figure 2. Sagittal uptake of ^{18}F-FDG in the abdominal aorta of rats on a normal diet and a high-fat diet at 16 and 24 weeks. Normal diet group at weeks (Aa) 16 and (Ab) 24. High-fat diet group at weeks (Ba) 16 and (Bb) 24. The arrows indicate the sagittal plane of the abdominal aorta. Comparison of average SUVs of abdominal aortic uptake of ^{18}F-FDG at weeks (Ca) 16 and (Cb) 24 in the normal diet group and the high-fat diet group. *$P<0.05$ vs. the control group. (Cc) Comparison of mean SUVs of abdominal aortic uptake of ^{18}F-FDG at 16 and 24 weeks in the high-fat diet group. *$P<0.05$ vs. the 16-week high-fat diet group. ^{18}F-FDG, ^{18}F-fluorodeoxyglucose; SUV, standardized uptake value.

normal diet group at 24 weeks, and on rats in the high-fat diet group at 16 and 24 weeks (Fig. 3A-C). Brown cells indicated macrophages with positive CD68 expression and revealed the aggregation of CD68-positive macrophages in the high-fat diet group (Fig. 3B and C). The staining intensity of CD68 was statistically analyzed by one-way ANOVA and Tukey's post hoc test. The percentage of CD68-positive cells in the total number of cells per unit area in each group was 3.20±1.80% in the normal diet group; 4.70±2.02% in the 16-week high-fat diet group; and 6.94±2.02% in the 24-week high-fat diet group. The percentage of CD68-positive cells was significantly higher in the 24-week high-fat diet group compared with in the 16-week high-fat diet group ($P<0.05$; Fig. 3D). In addition, the percentage of CD68-positive cells was significantly higher in the 24-week high-fat diet group compared with in the normal diet group at week 24 ($P<0.001$; Fig. 3D). The percentage of CD68-positive cells was higher in the 16-week high-fat diet

group compared with that in the normal diet group at week 24; however, there was no significant difference ($P>0.05$; Fig. 3D). These findings demonstrated that, with the increase in feeding time, the percentage of CD68-positive cells was increased in the aortic wall of rats on a high-fat diet, thus suggesting that the density of macrophages in the vascular wall of the abdominal aorta was increased with the increase in feeding time.

Discussion

Since the inflammatory hypothesis of atherosclerosis was proposed in 1999 (4), a growing number of studies have shown that monocytes, macrophages and vascular endothelial cells are involved in the inflammation of atherosclerosis, and macrophages have been reported to serve a critical role in the development and progression of atherosclerosis (17,18). Kubota *et al* (19) detected a higher uptake of ^{18}F-FDG in the cells around a
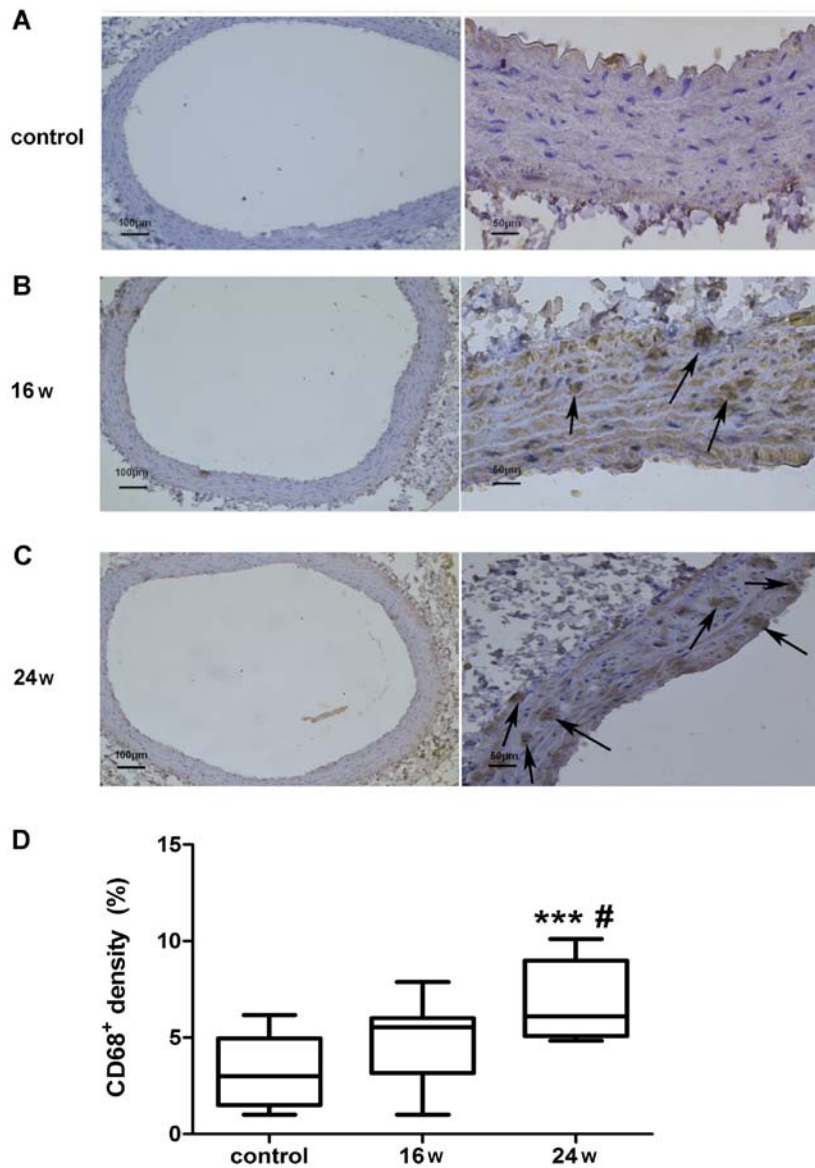
Figure 3. Expression of CD68-positive macrophages in the rat abdominal aortic wall. Immunohistochemical analysis of rat abdominal aortic vascular specimens, which were stained with CD68; the mean intensity of CD68 staining was analyzed. Arrows indicate the CD68^{+} cells. (A) Normal diet group at 24 weeks; (B) high-fat diet group at 16 weeks; (C) high-fat diet group at 24 weeks. (D) Percentage of CD68-positive cells in the total number of cells per unit area in each group were quantified: 3.20±1.72% for (A); 4.70±1.92% for (B); 6.93±1.93% for (C). Scale bars, 100 μm (left); 50 μm (right). Data are presented as the mean ± SEM. [***]P<0.001 vs. the normal diet (control) group; [#]P<0.05 vs. the 16-week group.

tumor compared with in viable tumor cells with high metabolic activity. A retrospective review of the records of 85 patients with cancer undergoing ^{18}F-FDG PET/CT demonstrated that ^{18}F-FDG uptake in the thoracic aortic wall may be correlated with the metabolic activity of atherosclerotic changes (20). In addition, ^{18}F-FDG accumulation has been shown to be caused by macrophage uptake, and it has been suggested that ^{18}F-FDG imaging may be used to provide a qualitative characterization of the inflammatory features of atherosclerosis and to quantify the degree of inflammation (10,21-24).

The present study detected significantly higher SUVs of ^{18}F-FDG in the iliac artery and abdominal aorta in the high-fat diet group compared with those in the normal diet group at 16 and 24 weeks, and a significantly greater SUV of ^{18}F-FDG in the arteries in the high-fat diet group at 24 weeks than at 16 weeks. These data indicated a significant increase in cellular metabolic activity in the vascular walls of the iliac artery and the abdominal aorta in the high-fat diet group compared with those in the normal diet group. Immunohistochemical staining detected accumulation of CD68-positive macrophages in the rat abdominal aortic wall in the high-fat diet group at 16 and 24 weeks; the 24-week high-fat diet groups exhibited significantly higher percentages of CD68-positive cells compared with in the normal diet group (P<0.001), and the percentage of CD68-positive cells was significantly higher in the 24-week high-fat diet group compared with that in the 16-week high-fat diet group (P<0.05). These results are similar to those of previous studies, which reported that ^{18}F-FDG uptake was strongly associated with macrophage density in atherosclerotic vessels (10,25-27). However, rabbits or mice were used in previous studies, whereas Wistar rats were used as an animal model in the present study (10,25-27).

Because rats have no gallbladder, feeding them with a high-fat diet does not easily induce a rise in cholesterol and produce atherosclerotic lesions (28,29). Therefore, atherosclerosis has been predominantly modeled in rabbits and mice. However, in previous studies in rat models of atherosclerosis, it has been reported that vitamin D + high-fat diet may induce atherosclerotic plaques (29-32). In the present study, inflammatory lesions of the arterial vessel walls were induced with a high-fat and high-salt diet in Wistar rats, and significantly higher body weight, abdominal circumference and Lee's index were detected in the high-fat diet group compared with those in the normal diet group at 8 weeks. In addition, significantly greater SBP and DBP were detected in the high-fat diet group than those in the normal diet group at 12 weeks, and significantly higher INS levels were revealed in the high-fat diet group than those in the normal diet group at 24 weeks, Conversely, there was no significant difference in fasting blood glucose between the two groups. In addition, rat blood pressure and body weight exhibited a consistent tendency: Body weight was shown to increase earlier than blood pressure, which was similar to previous findings demonstrating that rats with obesity induced by diet alone presented an increase in blood pressure after 12 weeks of feeding, and that elevated blood pressure may be associated with high-salt diet and obesity (33,34). Abdominal obesity has been accepted as the primary cause of INS resistance (27,32,35-38). In addition, in the present study, significantly higher TC levels were measured at 8 and 24 weeks, and a significantly higher LDL-C concentration was detected at 16 weeks in the high-fat diet group compared with in the normal diet group. Although pathological examinations did not detect typical atherosclerotic plaques, the aforementioned results indicated that ^{18}F-FDG uptake was increased in the rat iliac artery and abdominal aortic wall in the high-fat diet group compared with in the normal diet group, and that the SUV of ^{18}F-FDG was significantly higher in the high-fat diet group at 24 weeks than at 16 weeks. Taken together, these findings suggested that ^{18}F-FDG uptake may be associated with local macrophage accumulation, and the results of immunohistochemistry revealed that the increase in macrophage density was associated with the increase in ^{18}F-FDG uptake in arteries. These data are similar to previous studies reporting an association between the number of macrophages and the SUV of ^{18}F-FDG in mice (27). These findings also confirmed the successful modeling of inflammatory lesions of the arterial vessel walls induced by a high-fat and high-salt diet in Wistar rats.

Currently, most available imaging techniques used for the detection of atherosclerosis are based on the description of morphological features of atherosclerotic plaques, and there remains a lack of approaches for early diagnosis of atherosclerosis. Notably, there is a lack of non-invasive approaches that can be used for continuous monitoring of the range and degree of vascular wall inflammation. As a technique involving a combination of functional and structural imaging, PET/CT imaging has shown great potential in the assessment and diagnosis of atherosclerosis. ^{18}F-FDG activity has been reported to correlate with macrophage content within aortic atherosclerosis, and ^{18}F-FDG PET imaging may serve as a useful non-invasive imaging technique for the detection of atherosclerotic lesions (39). SUV is normally used to assess disease activity during PET imaging, which may provide quantitative

information on the severity of vascular wall inflammation for metabolic and structural imaging approaches. In animal models of atherosclerosis (mice or rabbits) receiving ^{18}F-FDG PET imaging, the metabolic activity of ^{18}F-FDG was shown to increase in activated macrophages, and a marked increase was detected in ^{18}F-FDG uptake in regions with macrophage activity (11). In addition, nanoparticle PET-CT imaging of macrophages in inflammatory atherosclerosis further revealed that the radionuclide activity of *in vivo* imaging was strongly correlated with macrophages in atherosclerotic plaques (11,40), and ^{18}F-FDG uptake has been reported to be proportional to the duration of cholesterol feeding, and to peak with plaque disruption and thrombosis (41).

In the current study, a Wistar rat model of vascular wall inflammation induced by a high-fat and high-salt diet was used. In this animal model, the arterial vessel walls were shown to display inflammatory lesions. This can also be said to be the early stage of atherosclerosis confirmed by the combination of ^{18}F-FDG PET and immunohistochemistry. The relationship between uptake of ^{18}F-FDG and inflammation has been demonstrated using histology linking ^{18}F-FDG uptake with the number of macrophages in arterial specimens (8,42,43). It may be hypothesized that although rats have no gallbladder and are resistant to atherosclerosis, their application prospects will improve if they can be developed and studied as an animal model of atherosclerosis. This is primarily because rats are low in cost, easily accessible, easy to feed and exhibit similar physiological anatomy to humans. In addition, compared with mice, rats are more suitable for the interventional study of drugs and instruments for endovascular angioplasty and stenting. Pahk *et al* (44) established a Sprague-Dawley rat model using right carotid artery ligation plus atherosclerosis diet and vitamin D injection. After 1 month, ^{18}F-FDG PET/CT indicated increased uptake of FDG in carotid atherosclerosis arteries, and the uptake in the inner layer was higher compared with that in the outer layer.

However, there are limitations in the present study: i) The rat model of the early inflammatory stage of atherosclerosis lacks evidence of inflammatory markers, such as leukocytes, high sensitivity C-reactive protein, myeloperoxidase, LI-6, monocyte chemoattractant protein-1, etc. ii) In addition, the results may be more meaningful if ultrasound was used to measure the thickness of the abdominal aorta and the feeding time was prolonged. Previous studies have revealed that ^{18}F-FDG PET/CT can specifically display inflammatory activity. For example, both human vascular tissue biopsy and animal studies have shown that ^{18}F-FDG intake is in direct proportion to the number of plaque macrophages (45), thus ^{18}F-FDG imaging can be used to identify unstable plaques. ^{18}F-FDG PET/CT can also detect atrial/auricular inflammation and is associated with stroke in patients with atrial fibrillation (46-48). Notably, ^{18}F-FDG PET/CT has unique and important value in the detection of a variety of types of cardiovascular inflammation. The present study assessed the establishment of an early inflammatory model of atherosclerosis in Wistar rats. The results revealed that ^{18}F-FDG PET might directly display the metabolic activity of macrophage accumulation in local arterial vessel walls in Wistar rats. These data demonstrated that ^{18}F-FDG PET imaging may be considered a feasible method to detect inflammatory lesions of the arterial vessel walls in Wistar rats. It was therefore hypothesized that stable modeling of atherosclerosis

in Wistar rats by vitamin D treatment + intima injury and extension of the feeding duration of the high-fat and high-salt diet (29-32,44), which may strengthen the characteristics of the Wistar rat atherosclerosis model (arterial intima thickness, vascular wall plaque formation and vascular lumen stenosis), followed by ^{18}F-FDG PET imaging, may provide imaging data support for the early identification, non-invasive assessment and dynamic monitoring of atherosclerosis.

Acknowledgements

Funding

Availability of data and materials

The datasets used and/or analyzed during the current study are available from the corresponding author on reasonable request.

Authors' contributions

SS conceived and designed the study, drafted the manuscript, interpreting data and revised important academic contents; HL conceived and designed the study, drafted the manuscript, analyzed physiological and biochemical data; SG drafted the manuscript, interpreting data and revised important academic content; HH performed PET detection and data collection; HZ performed pathological examination and data collection; FL performed physiological data recording and data collection; YF collected the vascular specimens of rats and analyzed the PET and pathological test data; LW performed feeding and physiological data acquisition of rats; XW performed blood biochemical detection and data collection; YL conceived and designed the study, interpreted the data, modified important academic content and gave final approval to the publication of this edition; ZS conceived and designed the study, analyzed and interpreted data, modified important academic content and gave final approval to the publication of this edition. All authors read and approved the final manuscript.

Ethics approval and consent to participate

This study was approved by the Ethics Review Committee of Jiangsu Lake Taihu Sanatorium (Permission number: SGLERC-2011008; Wuxi, China) and Jiangsu Provincial People's Hospital Group (Permission number: SRY20100820).

Patient consent for publication

Not applicable.

Competing interests

The authors declare that they have no competing interests.

References

1. National Center for Cardiovascular Disease: China. Report on Cardiovascular disease in China (2016). Encyclopedia of China Publishing House, Beijing, 2017.
2. Roth GA, Johnson C, Abajobir A, Abd-Allah F, Abera SF, Abyu G, Ahmed M, Aksut B, Alam T, Alam K, *et al*: Global, regional and national burden of cardiovascular diseases for 10 causes, 1990 to 2015. J Am Coll Cardiol 70: 1-25, 2017.
3. McKenney-Drake ML, Moghbel MC, Paydary K, Alloosh M, Houshmand S, Moe S, Salavati A, Sturek JM, Territo PR, Weaver C, *et al*: ^{18}F-NaF and ^{18}F-FDG as molecular probes in the evaluation of atherosclerosis. Eur J Nucl Med Mol Imaging 45: 2190-2200, 2018.
4. Ross R: Atherosclerosis - an inflammatory disease. N Engl J Med 340: 115-126, 1999.
5. Fan LM: Rethinking the pathogenesis of atherosclerosis. Chin J Arterioscler 13: 249-253, 2005.
6. Hosono M, de Boer OJ, van der Wal AC, van der Loos CM, Teeling P, Piek JJ, Ueda M and Becker AE: Increased expression of T cell activation markers (CD25, CD26, CD40L and CD69) in atherectomy specimens of patients with unstable angina and acute myocardial infarction. Atherosclerosis 168: 73-80, 2003.
7. Chen W, Bural GG, Torigian DA, Rader DJ and Alavi A: Emerging role of FDG-PET/CT in assessing atherosclerosis in large arteries. Eur J Nucl Med Mol Imaging 36: 144-151, 2009.
8. Wang ZJ, Deng G, Huang HB, Li AM, Ju SH, Zhao R, Jin H and Wei XY: Noninvasive observation of atherosclerosis in mice with 7.0T MR and Micro-PET. Chin J Med Imaging Technol 26: 209-212, 2010.
9. Ogawa M, Ishino S, Mukai T, Asano D, Teramoto N, Watabe H, Kudomi N, Shiomi M, Magata Y, Iida H, *et al*: (18)F-FDG accumulation in atherosclerotic plaques: Immunohistochemical and PET imaging study. J Nucl Med 45: 1245-1250, 2004.
10. Tawakol A, Migrino RQ, Hoffmann U, Abbara S, Houser S, Gewirtz H, Muller JE, Brady TJ and Fischman AJ: Noninvasive in vivo measurement of vascular inflammation with F-18 fluorodeoxyglucose positron emission tomography. J Nucl Cardiol 12: 294-301, 2005.
11. Feng TT and Zhao QM: Advances of PET/CT in noninvasive assessing of atherosclerosis plaque. Chin J Med Imaging Technol 26: 971-973, 2010.
12. Lau AZ, Miller JJ, Robson MD and Tyler DJ: Cardiac perfusion imaging using hyperpolarized (13)C urea using flow sensitizing gradients. Magn Reson Med 75: 1474-1483, 2016.
13. Di Cesare Mannelli L, Micheli L, Carta F, Cozzi A, Ghelardini C and Supuran CT: Carbonic anhydrase inhibition for the management of cerebral ischemia: In vivo evaluation of sulfonamide and coumarin inhibitors. J Enzyme Inhib Med Chem 31: 894-899, 2016.
14. Pan L, Yang F, Lu C, Jia C, Wang Q and Zeng K: Effects of sevoflurane on rats with ischemic brain injury and the role of the TREK-1 channel. Exp Ther Med 14: 2937-2942, 2017.
15. Li S, *et al*: Comparative study on anesthetic role of chloral hydrate on rat. Drug Res 23: 22-23, 2014.
16. Wang JF: Guidelines for the Management and Use of Laboratory Animals. Shanghai Science and Technology Press, 2012.
17. Tabas I and Bornfeldt KE: Macrophage phenotype and function in different stages of atherosclerosis. Circ Res 118: 653-667, 2016.
18. Zhang Y, Zhang C and Zhang M: A new era of anti-inflammatory therapy for atherosclerosis. Zhonghua Xin Xue Guan Bing Za Zhi 46: 332-337, 2018 (In Chinese).
19. Kubota R, Yamada S, Kubota K, Ishiwata K, Tamahashi N and Ido T: Intratumoral distribution of fluorine-18-fluorodeoxyglucose in vivo: High accumulation in macrophages and granulation tissues studied by microautoradiography. J Nucl Med 33: 1972-1980, 1992.

20. Tatsumi M, Cohade C, Nakamoto Y and Wahl RL: Fluorodeoxyglucose uptake in the aortic wall at PET/CT: Possible finding for active atherosclerosis. Radiology 229: 831-837, 2003.

21. Cullen P, Baetta R, Bellosta S, Bernini F, Chinetti G, Cignarella A, von Eckardstein A, Exley A, Goddard M, Hofker M, et al; MAFAPS Consortium: Rupture of the atherosclerotic plaque: Does a good animal model exist? Arterioscler Thromb Vasc Biol 23: 535-542, 2003.

22. Ogawa M, Magata Y, Kato T, Hatano K, Ishino S, Mukai T, Shiomi M, Ito K and Saji H: Application of 18F-FDG PET for monitoring the therapeutic effect of antiinflammatory drugs on stabilization of vulnerable atherosclerotic plaques. J Nucl Med 47: 1845-1850, 2006.

23. Matter CM, Wyss MT, Meier P, Späth N, von Lukowicz T, Lohmann C, Weber B, Ramirez de Molina A, Lacal JC, Ametamey SM, et al: 18F-choline images murine atherosclerotic plaques ex vivo. Arterioscler Thromb Vasc Biol 26: 584-589, 2006.

24. Zhao QM, Feng TT, Zhao X, Xu ZM, Liu Y, Li DP, Li LQ, Su G and Zhang XX: Imaging of atherosclerotic aorta of rabbit model by detection of plaque inflammation with fluorine-18 fluorodeoxyglucose positron emission tomography/computed tomography. Chin Med J (Engl) 124: 911-917, 2011.

25. Knesaurek K, Machac J, Vallabhajosula S and Buchsbaum MS: A new iterative reconstruction technique for attenuation correction in high-resolution positron emission tomography. Eur J Nucl Med 23: 656-661, 1996.

26. Lederman RJ, Raylman RR, Fisher SJ, Kison PV, San H, Nabel EG and Wahl RL: Detection of atherosclerosis using a novel positron-sensitive probe and 18-fluorodeoxyglucose (FDG). Nucl Med Commun 22: 747-753, 2001.

27. Wang XN, et al: Application of 18F-FDG nuclide imaging of atherosclerotic plaques in apolipoprotein E-deficient mice. J Chin PLA Postgrad Med Sch 6: 645-647, 2011.

28. Wang HR and Yu CJ: New progress in mechanism and treatment of atherosclerosis. J Cap Med Univ 31: 828-833, 2010.

29. Zhang YL, et al: Method of establishment of model of experimental atherosclerosis in rats. J Wenzhou Med Coll 37: 331-333, 2007.

30. Xue YQ and Huang SA: A fast method of establishment of atherosclerotic rat model. Med Innov Chin 11: 1-4, 2014.

31. Zhou H, Wu XY, Yuan YB and Qi XH: Comparison of methods for establishing a rat model of atherosderosis using three-doses of Vitamin D3 and atherogenic diet. Chin J Arterioscler 20: 995-998, 2012.

32. Guo YS, et al: Comparison on the three duplication methods of atherosclerosis model in rat. Chin J Arterioscler 11: 465-469, 2003.

33. Hu H, Xu Y, Liu C, Zhao H, Zhang H and Wang L: Changes in behavior and in brain glucose metabolism in rats after nine weeks on a high fat diet: A randomized controlled trial. Shanghai Arch Psychiatry 26: 129-137, 2014.

34. Dobrian AD, Davies MJ, Prewitt RL and Lauterio TJ: Development of hypertension in a rat model of diet-induced obesity. Hypertension 35: 1009-1015, 2000.

35. Hamman RF: Genetic and environmental determinants of non-insulin-dependent diabetes mellitus (NIDDM). Diabetes Metab Rev 8: 287-338, 1992.

36. Tankó LB, Bagger YZ, Alexandersen P, Larsen PJ and Christiansen C: Peripheral adiposity exhibits an independent dominant antiatherogenic effect in elderly women. Circulation 107: 1626-1631, 2003.

37. Chen J: Dietary capsaicin prevents insulin resistance in high fat diet-induced mice. Di 3 Jun Yi Da Xue Xue Bao 35: 585-588, 2013 (In Chinese).

38. Alexander RW: President's address. Common mechanisms of multiple diseases: Why vegetables and exercise are good for you. Trans Am Clin Climatol Assoc 121: 1-20, 2010.

39. Zhang Z, Machac J, Helft G, Worthley SG, Tang C, Zaman AG, Rodriguez OJ, Buchsbaum MS, Fuster V and Badimon JJ: Non-invasive imaging of atherosclerotic plaque macrophage in a rabbit model with F-18 FDG PET: A histopathological correlation. BMC Nucl Med 6: 3, 2006.

40. Nahrendorf M, Zhang H, Hembrador S, Panizzi P, Sosnovik DE, Aikawa E, Libby P, Swirski FK and Weissleder R: Nanoparticle PET-CT imaging of macrophages in inflammatory atherosclerosis. Circulation 117: 379-387, 2008.

41. Aziz K, Berger K, Claycombe K, Huang R, Patel R and Abela GS: Noninvasive detection and localization of vulnerable plaque and arterial thrombosis with computed tomography angiography/positron emission tomography. Circulation : 2061-2070, 2008.

42. Bucerius J, Dijkgraaf I, Mottaghy FM and Schurgers LJ: Target identification for the diagnosis and intervention of vulnerable atherosclerotic plaques beyond 18F-fluorodeoxyglucose positron emission tomography imaging: Promising tracers on the horizon. Eur J Nucl Med Mol Imaging 46: 251-265, 2019.

43. Tawakol A, Migrino RQ, Bashian GG, Bedri S, Vermylen D, Cury RC, Yates D, LaMuraglia GM, Furie K, Houser S, et al: In vivo 18F-fluorodeoxyglucose positron emission tomography imaging provides a noninvasive measure of carotid plaque inflammation in patients. J Am Coll Cardiol 48: 1818-1824, 2006.

44. Pahk K, Joung C, Jung SM, Young Song H, Yong Park J, Woo Byun J, Lee YS, Chul Paeng J, Kim C, Kim S, et al: Visualization of synthetic vascular smooth muscle cells in atherosclerotic carotid rat arteries by F-18 FDG PET. Sci Rep 7: 6989, 2017.

45. Evans NR, Tarkin JM, Chowdhury MM, Warburton EA and Rudd JH: PET imaging of atherosclerotic disease: Advancing plaque assessment from anatomy to pathophysiology. Curr Atheroscler Rep 18: 30, 2016.

46. Yang MF: Advancing the clinical application of (18) F-fluorodeoxyglucose positron emission tomography/computed tomography in cardiovascular inflammation. Zhonghua Xin Xue Guan Bing Za Zhi 48: 181-185, 2020 (In Chinese).

47. Xie B, Chen BX, Wu JY, Liu X and Yang MF: Factors relevant to atrial 18F-fluorodeoxyglucose uptake in atrial Fibrillation. J Nucl Cardiol 27: 1501-1512, 2018.

48. Sinigaglia M, Mahida B, Piekarski E, Chequer R, Mikail N, Benali K, Hyafil F, Le Guludec D and Rouzet F: FDG atrial uptake is associated with an increased prevalence of stroke in patients with atrial fibrillation. Eur J Nucl Med Mol Imaging 46: 1268-1275, 2019.